From Discrete Metal−Oxygen Clusters to Open-Framework Structure: Syntheses and Characterization of $Cs_2Mo_2O_5As_2O_7 \cdot H_2O$, $Cs_2Mo_2O_5(HAsO_4)_2 \cdot H_2O$, and $Cs_4Mo_6O_{18}(H_2O)(HAsO_4)_2 \cdot 2.5H_2O$

Kuei-Fang Hsu and Sue-Lein Wang*

Department of Chemistry, National Tsing Hua University, Hsinchu, Taiwan 30043

Received December 11, 1997

Three new molybdenum(VI) arsenate hydrates, $Cs_2Mo_2O_5As_2O_7 \cdot H_2O$ (**1**), $Cs_2Mo_2O_5(HAsO_4)_2 \cdot H_2O$ (**2**), and $Cs_4Mo_6O_{18}(H_2O)(HAsO_4)_2 \cdot 2.5H_2O$ (**3**), have been prepared and structurally characterized by single-crystal X-ray diffraction, thermal analysis, and IR spectroscopy. Crystal data: **1**, monoclinic, $P2_1/c$ $a = 7.9783(5)$ Å, $b = 10.7837(6)$ Å, $c = 15.5213(9)$ Å, $\beta = 93.594(1)°$, and $Z = 4$; **2**, triclinic, $P\bar{1}$, $a = 7.8165(2)$ Å, $b = 9.8902(3)$ Å, $c = 11.0401(3)$ Å, $\alpha = 63.814(1)°$, $\beta = 70.475(1)°$, $\gamma = 72.655(1)°$, $Z = 2$; **3**, monoclinic, $P2_1/n$, $a = 8.0345(1)$ Å, $b = 20.0364(4)$ Å, $c = 19.5941(3)$ Å, $\beta = 92.296(1)°$, $Z = 4$. Crystal **1** adopts an open framework structure which contains vertex-sharing bioctahedral Mo_2O_{11} units linked by $As_2O_7^{4-}$ groups to form intersecting tunnels where Cs^+ cations and water molecules reside. Crystals **2** and **3** are composed of the discrete cluster anions, $[Mo_4O_{10}(HAsO_4)_4]^{4-}$ and $[Mo_6O_{18}(H_2O)(HAsO_4)_2]^{4-}$, respectively. These anions are held in space via the interactions with Cs^+ cations and hydrogen bonds. Thermal studies showed both crystals **2** and **3** are transformed into **1** upon prolonged heating. It exhibits the first experimental evidence that a metal diarsenate framework can be converted thermally from hydrogen arsenate-containing polyanions. The three compounds are the first members prepared in the $Cs/Mo^{VI}/As^{V}/O$ system.

Introduction

Recently microporous solids containing transition elements have aroused much attention for their novel catalytic and magnetic properties which are not accessible to the main group systems of tetrahedral framework zeolites. The microporous behavior was successfully extended into a large class of novel octahedral−tetrahedral framework materials characterized in titanium silicates[1] and the phosphate systems of vanadium, iron, and molybdenum.[2] Syntheses of these materials usually involved organic templates for generating large cavities and were performed under mild hydrothermal conditions to avoid the tendency to yield dense phases. Recently, Haushalter and coworkers[3] obtained a novel framework, which bears an extremely low framework-metal-atom density, by using the alkaline metal Cs^+cations as a templating agent. We have been interested in the synthesis of new open-framework structures involving inorganic cations as structure-directing agents and have hydrothermally prepared a few remarkable transition metal arsenate compounds.[4] Here, we report the flux-growth mediated self-assembly and single-crystal structures of the first tridimensional molybdenum(VI) diarsenate, $Cs_2Mo_2O_5As_2O_7 \cdot H_2O$ (**1**), and two new polyanion-containing compounds, $Cs_2Mo_2O_5(HAsO_4)_2 \cdot H_2O$ (**2**) and $Cs_4Mo_6O_{18}(H_2O)(HAsO_4)_2 \cdot 2.5H_2O$ (**3**). Crystals of **1** contains large cavities and tunnels with the framework-metal-atom density comparable to the phosphate mineral cacoxenite.[5] Interestingly, the three-dimensional network of **1** can be respectively generated from the discrete cluster anions in **2** and **3**. In this paper, the syntheses, thermal studies, IR data, and detailed crystal structures are presented.

Experimental Section

Synthesis and Thermal Analysis. The three title compounds were first discovered in the order of **2**, **3**, and **1**. Hydrothermal treatment of CsOH (5 mmol), MoO_2 (1 mmol), H_3AsO_4 (20 mmol), H_2O (9.5 mL), and 0.2 mL of Et_2NH for 4 days at 200 °C yielded colorless equant crystals of **2** and a small amount of black powders of unreacted MoO_2. The TG curve showed weight loss in three steps (Figure 1): the release of lattice H_2O from ∼40 to ∼150 °C, the dehydration of $HAsO_4^{2-}$ groups from ∼260 to ∼380 °C, and the sublimation of MoO_3 corresponding to the sharp fall beginning at ∼740 °C. The observed total weight loss of 4.5% for the first two steps agrees well with the calculated value of 4.3% for $2H_2O$. Between the temperature range from ∼400 to 650 °C, no weight loss corresponding to further decomposition of the arsenate groups was detected. However, a broad endothermic peak appeared at ca. 465 °C in the DT curve, indicating the emergence of a new phase. A sample of **2** was accordingly heated at 500 °C for 4 h in air and quenched to room temperature. On the basis of powder X-ray analysis, the thermal product of **2** gave a pure phase of **1** (vide infra). The flux-growth method was then chosen to further pursue the crystal growth of **1**.

A mixture of CsH_2AsO_4 (0.1091 g, 4 mmol), $NH_4H_2AsO_4$ (0.0318 g, 2 mmol), and MoO_3 (0.0864 g, 6 mmol) was ground in an agate mortar, placed in a 3 mL platinum crucible, and heated from room temperature to 600 °C for 12 h, followed by a slow cooling (5 °C h^{-1})

(1) (a) Kuznicki, S. M.; Thrush, K. A.; Allen, F. M.; Levine, S. M.; Kamil, M. M.; Hayhurst, D. T.; Mansour, M. S. *Microporous Mater*. **1992**, *1*, 427. (b) Poojary, D. M.; Cahill, R. A.; Clearfield, A. *Chem. Mater*. **1994**, *6*, 2364.

(2) (a) Haushalter, R. C.; Mundi, L. A. *Chem. Mater*. **1992**, *4*, 31. (b) Guesdon, A.; Borel, M. M.; Leclaire, A.; Grandin, A.; Raveau, B. *J. Solid State Chem*. **1994**, *111*, 315. (c) Lii, K. H.; Huang, Y. F. *J. Chem. Soc., Chem. Commun*. **1997**, *13*, 222.

(3) Khan, M. I.; Meyer, L. M.; Haushalter, R. C.; Schweitzer, A. L.; Zubieta, J.; Dye, J. L. *Chem. Mater*. **1996**, *8*, 43.

(4) (a) Cheng, C. Y.; Wang, S. L. *J. Chem. Soc., Dalton Trans* **1992**, 2395. (b) Wang, S. L.; Lee, Y. H. *Inorg. Chem*. **1994**, *33*, 3845. (c) Fan, N. Y.; Wang, S. L. *Inorg. Chem*. **1996**, *35*, 4708. (d) Hsu, K. F.; Wang, S. L. *Inorg. Chem*. **1997**, *36*, 3049.

(5) Moore, P. B.; Shen, J. *Nature* **1983**, *306*, 356.

S0020-1669(97)01562-0 CCC: $15.00
Published on Web 06/09/1998

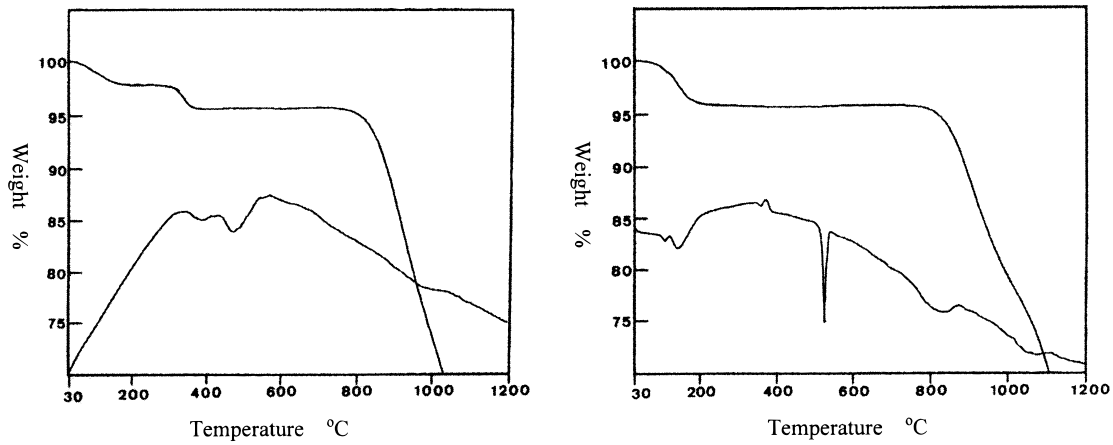

Figure 1. Thermal analysis of $Cs_2Mo_2O_5(HAsO_4)_2 \cdot H_2O$ (left) and $Cs_4Mo_6O_{18}(H_2O)(HAsO_4)_2 \cdot 2H_2O$ (right): the upper traces are TG curves, and the lower traces are DT curves.

Scheme 1

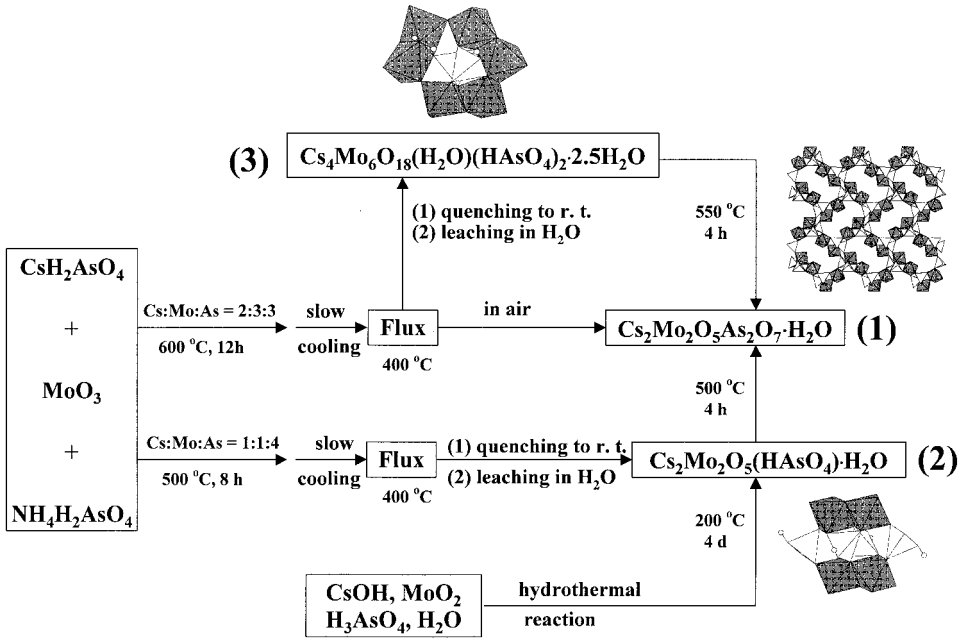

to 400 °C and quenched to room temperature on removal of the crucible from the furnace. The flux was dissolved in boiling water and a solid product was obtained by suction filtration. The product contained a single phase of colorless rodlike crystals of $Cs_4Mo_6O_{18}(H_2O)(HAsO_4)_2 \cdot 2.5H_2O$ (**3**). In the TG curve shown in Figure 1, a weight loss of 4.4% occurred between ~50 and 240 °C which agrees well with the calculated value of 4.66% for $4.5H_2O$. It was noted that the TG curve of the dehydration of **3** behaved the same as that of **2**. In addition, a sharp endothermic peak at ca. 525 °C occurred in the DT curve without any counterpart in the TG curve as well. A sample of **3** was then heated at 550 °C for 4 h in air and quenched to room temperature. As indicated by powder XRD patterns, the thermal product of **3** contained **1** as well. This result led us to reproduce the flux without leaching. Finally, a small amount of tiny colorless crystals of **1** were scrutinized from the pulverulent flux. In the course of the study, efforts were also made to prepare **2** by flux method. After many attempts, **2** was successfully obtained as a single phase by heating a mixture of CsH_2AsO_4 (0.6 mmol), $NH_4H_2AsO_4$ (1.8 mmol), and MoO_3 (0.6 mmol) at 500 °C for 8 h. The preparation of all three compounds are outlined in Scheme 1.

Single-Crystal X-ray Structure Analysis. Crystal structures of the three title compounds were determined by single-crystal X-ray diffraction methods. The procedures for **1** are given in the following. A tiny crystal of **1** of dimensions 0.03 × 0.03 × 0.05 mm was selected for indexing and intensity data collection on a Siemens Smart-CCD diffractometer equipped with a normal focus, 3 kW sealed-tube X-ray source ($\lambda = 0.710\ 73$ Å). Intensity data were collected in 1271 frames with increasing ω (width of 0.3° per frame). Unit cell dimensions were determined by a least-squares fit of 3436 reflections. Of the 7875 reflections ($2\theta_{max} = 56.75°$), 5968 unique reflections ($R_{int} = 0.041$) were considered observed ($I > 3\sigma(I)$) after *Lp* and absorption corrections. The absorption correction was based on symmetry-equivalent reflections using the *SADABS* program.[6] On the basis of systematic absences and statistics of intensity distribution, the space group for **1** was determined to be $P2_1/c$. Direct methods were used to locate the metal, arsenic, and a few oxygen atoms, the remaining non-hydrogen atoms being found from successive difference maps. The two water hydrogen atoms were located on a difference Fourier map calculated at the final stage of structure analysis. The final cycle of refinement, including the atomic coordinates and anisotropic thermal parameters for all non-hydrogen atoms and fixed atomic coordinates and isotropic thermal parameters for H atoms, converged at $R = 0.0378$ and $R_w = 0.0325$. In the final difference map the deepest hole was -1.62 e Å^{-3} and the highest peak 1.34 e Å^{-3}. Corrections for secondary extinction and anomalous dispersion were applied. Neutral-atom scattering factors were used. Structure solution and least-squares

(6) Sheldrick, G. M. *SADABS*; Siemens Analytical X-ray Instrument Division: Madison, WI, 1995.

Table 1. Crystallographic Data

	1	**2**	**3**
empirical formula	$H_2As_2Cs_2Mo_2O_{13}$	$H_4As_2Cs_2Mo_2O_{14}$	$H_8As_2Cs_4Mo_6O_{29}$
fw	817.6	835.6	1738.1
space group	$P2_1/c$	$P\bar{1}$	$P2_1/n$
a, Å	7.9783(5)	7.8165(2)	8.0345(1)
b, Å	10.7837(6)	9.8902(3)	20.0364(4)
c, Å	15.5213(9)	11.0401(3)	19.5941(3)
α, deg	90	63.814(1)	90
β, deg	93.594(1)	70.475(1)	92.296(1)
γ, deg	90	72.655(1)	90
V, Å^3	1332.8(4)	710.3(3)	3151.8(9)
Z	4	2	4
ρ_{calcd}, gcm^{-3}	4.074	3.907	3.662
μ, cm^{-1}	122.52	115.04	90.52
T, °C	21	21	21
λ, Å	0.710 73	0.710 73	0.710 73
$R(F_o)^a$	0.0378	0.0408	0.0448
$R_w(F_o)^b$	0.0325	0.0459	0.0406

^{a} $R = \sum||F_o| - |F_c||/\sum|F_o|$. ^{b} $R_w = [\sum(|F_o| - |F_c|)^2/\sum w|F_o|^2]^{1/2}$, $w = 1/\sigma^2(F_o)$ for **1** and **2**, $w = [\sigma^2(F_o) + gF_o^2]^{-1}$ for **3**, $g = 0.00005$.

Table 2. Atomic Coordinates[a] and Thermal Parameters (Å^2) for $Cs_2MO_2O_5As_2O_7 \cdot H_2O$ (**1**)

atom	x/a	y/b	z/c	U_{eq}[b]
Cs(1)	0.34471(9)	0.18639(7)	0.91856(5)	0.0287(3)
Cs(2)[c]	−0.12596(16)	0.41311(28)	0.83511(11)	0.0505(7)
Cs(2A)[c]	−0.12367(84)	0.48069(114)	0.85561(52)	0.0505(7)
Mo(1)	0.82574(11)	0.30083(9)	0.54035(6)	0.0171(3)
Mo(2)	0.63857(12)	0.08646(9)	0.67983(6)	0.0179(3)
As(1)	0.50169(13)	0.38070(10)	0.67812(7)	0.0161(4)
As(2)	0.14753(13)	0.49184(10)	0.62689(7)	0.0156(4)
O(1)	0.5242(9)	0.5130(7)	0.7353(5)	0.022(3)
O(2)	0.6060(9)	0.3966(7)	0.5908(4)	0.020(3)
O(3)	0.5487(9)	0.2596(7)	0.7393(5)	0.022(3)
O(4)	0.2889(9)	0.3662(6)	0.6443(4)	0.016(2)
O(5)	0.1975(9)	0.6008(7)	0.6990(5)	0.025(3)
O(6)	0.1851(9)	0.5339(7)	0.5263(4)	0.020(2)
O(7)	−0.0394(8)	0.4299(7)	0.6366(4)	0.020(3)
O(8)	0.7296(9)	−0.0519(7)	0.6592(5)	0.027(3)
O(9)	0.4858(10)	0.0990(8)	0.5996(5)	0.032(3)
O(10)	0.8056(9)	0.1941(7)	0.6373(4)	0.019(2)
O(11)	0.6957(9)	0.2255(7)	0.4678(5)	0.023(3)
O(12)	1.0165(9)	0.2552(7)	0.5089(5)	0.027(3)
O(13)	0.1206(12)	0.1864(11)	0.7483(6)	0.072(5)
H(13A)	0.15987	0.23187	0.69683	0.05
H(13B)	0.00237	0.18427	0.74013	0.05

[a] Atomic coordinates and thermal parameters for compunds **2** and **3** are given in the Supporting Information. [b] U_{eq} is defined as one-third of the trace of the orthogonalized $\mathbf{U}_{ij}$ tensor. [c] The occupancy factors are 80% and 20% for the Cs(2) and the Cs(2a) sites, respectively.

refinements were performed on a DEC VAX 4000/90 workstation using the *SHELXTL-Plus* programs.[7]

Results and Discussion

The crystallographic data are listed in Table 1, atomic coordinates and thermal parameters are in Table 2, and selected bond lengths and bond valence sums[8] are in Table 3. The Mo and As atoms are six- and four-coordinated, respectively. The coordination numbers of the Cs atoms in **1**, **2**, and **3**, ranging from 8 to 10, were determined on the basis of the maximum gap in the Cs−O distances ranked in increasing order. The maximum cation−oxygen distance, $L_{max} = 3.60$ Å for Cs−O, according to Donnay and Allmann,[9] was also considered.

Table 3. Selected Bond Distances (Å) and Bond Valence Sums ($\sum s$) for $Cs_2MO_2O_5As_2O_7 \cdot H_2O$ (**1**)[a]

Cs(1)−O(11)[a]	3.010(7)	Cs(2)−O(11)[b]	2.980(8)
Cs(1)−O(13)	3.097(10)	Cs(2)−O(8)[c]	3.179(8)
Cs(1)−O(12)[b]	3.111(7)	Cs(2)−O(7)	3.208(7)
Cs(1)−O(8)[c]	3.112(7)	Cs(2)−O(13)[c]	3.210(12)
Cs(1)−O(2)[d]	3.154(7)	Cs(2)−O(1)[e]	3.287(7)
Cs(1)−O(6)[a]	3.213(7)	Cs(2)−O(3)[e]	3.354(7)
Cs(1)−O(1)[d]	3.255(7)	Cs(2)−O(12)[b]	3.390(8)
Cs(1)−O(3)	3.404(7)	Cs(2)−O(5)[f]	3.463(8)
Cs(1)−O(2)[a]	3.405(7)	Cs(2)−O(13)	3.474(11)
$\sum s$[Cs(1)−O] = 1.16		$\sum s$[Cs(2)−O] = 0.94	
Mo(1)−O(11)	1.692(7)	Mo(2)−O(9)	1.692(7)
Mo(1)−O(12)	1.701(7)	Mo(2)−O(8)	1.699(7)
Mo(1)−O(10)	1.908(7)	Mo(2)−O(10)	1.916(7)
Mo(1)−O(6)[g]	2.060(7)	Mo(2)−O(1)[d]	2.065(7)
Mo(1)−O(2)	2.219(7)	Mo(2)−O(3)	2.223(7)
Mo(1)−O(7)[h]	2.265(7)	Mo(2)−O(5)[d]	2.228(7)
$\sum s$[Mo(1)−O] = 6.00		$\sum s$[Mo(2)−O] = 6.02	
As(1)−O(1)	1.684(7)	As(2)−O(4)	1.772(7)
As(1)−O(2)	1.644(7)	As(2)−O(5)	1.655(7)
As(1)−O(3)	1.643(7)	As(2)−O(6)	1.671(7)
As(1)−O(4)	1.753(7)	As(2)−O(7)	1.648(7)
$\sum s$[As(1)−O] = 5.08		$\sum s$[As(2)−O] = 5.02	
O(13)−H(13A)	1.004	O(13)−H(13B)	0.944

[a] Symmetry codes: (a) x, 1/2 − y, 1/2 + z; (b) −1 + x, 1/2 − y, 1/2 + z; (c) 1-x, 1/2 + y, 3/2 − z; (d) 1 − x, −1/2 + y, 3/2 − z; (e) −1 + x, y, z; (f) -x, −1/2 + y, 3/2 − z; (g) 1-x, 1-y, 1-z; (h) 1 + x, y, z.

A projection of the structure of **1** along the [100] direction is shown in Figure 2. It adopts an original structure in which the three-dimensional network is built up from corner-sharing bioctahedral Mo_2O_{11} units and As_2O_7 groups. According to our literature search, structurally characterized molybdenum(VI) diarsenate compounds are rare. Besides the potassium compound $K_2MoO_2(MoO_2As_2O_7)_2$,[10] **1** becomes the second tridimensional diarsenate compound in the $Mo^{VI}/As^{V}/O$ lattices. As shown in Figure 2, the fundamental building units involve two Mo_2O_{11} bioctahedra and two As_2O_7 groups. Each of the eight-membered units is joined by corner-sharing, via −As(2)−O(7)−Mo(1)− bonds, to others forming infinite columns running parallel to the [100] direction. The infinite columns lie on inversion centers and share corners with *c*-glide symmetry-related ones to generate large tunnels. The tunnel openings are 10-ring windows formed by the edges of six MoO_6 octahedra and four AsO_4 tetrahedra. Lateral windows with smaller sizes can be observed in the [010] and [001] directions as well.

Structure **1** may be alternatively viewed as stacking of the macroanionic nets, shown in Figure 3, running parallel to the (102) planes. The nets, each with a thickness of ∼5.9 Å, are comprised of 14-membered rings formed by eight MoO_6 octahedra and six AsO_4 tetrahedra. The long side of the ring has a free dimension (minimum O···O distance less one O diameter of 2.6 Å) of 12.5 Å. Stackings of such porous nets result in large cavities which are interconnected to form open tunnels undulating through the framework. Atom Cs(1) is located at the intersections of three-way tunnels. Cs(2), disordered over two sites, is located at the intersections of two-way tunnels. The lattice water molecules, weakly bonded to both Cs(1) and Cs(2), are confined within the open windows

(7) Sheldrick, G. M. *SHELXTL-Plus Crystallographic System*, Release 4.21; Siemens Analytical X-ray Instrument Division: Madison, WI, 1991.
(8) Brown, I. D.; Altermatt, D. *Acta Crystallogr*. **1985**, *B41*, 244.
(9) Donnay, G.; Allmann, R. *Am. Mineral*. **1970**, *55*, 1003.
(10) Zid, M. F.; Jouini, T. *Acta Crystallogr., Sect. C* **1996**, *52*, 2947.

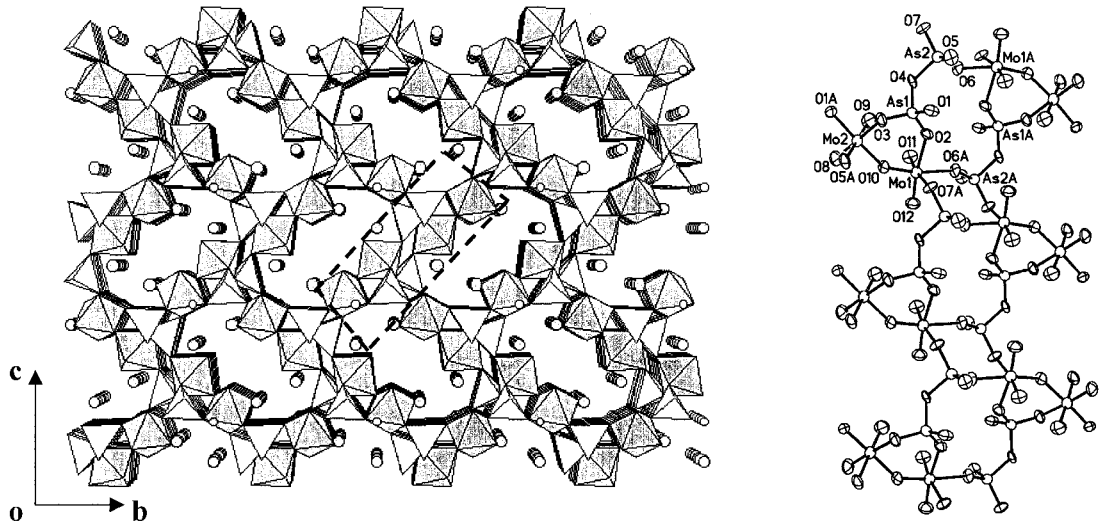

Figure 2. Structure plots of **1**. (Left) Polyhedron representation of the framework, with the fundamental building unit marked in dashed rectangle. In the drawing, the corners of polyhedra are O atoms and the Mo and As atoms are at the center of each octahedron and tetrahedron, respectively. The dark stippled polyhedra represent MoO_6, the light tetrahedra As_2O_7 groups, the large stippled circles carbons, and the small open circles water oxygens. (Right) ORTEP drawing (50% ellipsoids) of section of an infinite column formed by the eight-membered building units (also see text) along with atomic labeling.

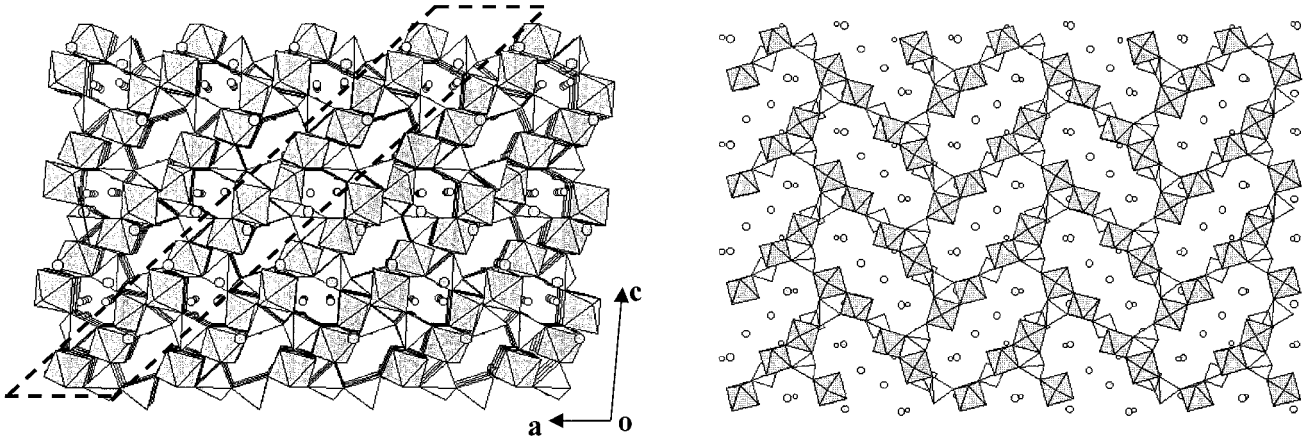

Figure 3. Structure of **1** is viewed as stacking of the macroanionic nets, as marked in dashed lines, running parallel to the (102) planes. Section of the net showing the 14-membered rings with atom-to-atom diameter of 15.1 Å is shown in the right.

of the nets. One of the most striking features of **1** is the large empty interstitial space inside the network, which is also reflected in the very low framework-metal-atom density (FD), 12.0 M atoms (M = Mo, As)/1000 Å^3, as compared with the value of 12.7 M atoms/1000 Å^3 for the very open faujasite (M = Si),[11] and 12.1 M atoms/1000 Å^3 for the phosphate mineral cacoxenite.[5] Another feature lies in the vertex-sharing Mo_2O_{11} units; although they are not uncommonly seen in reduced molybdenum phosphates,[12] they seldom occur in the Mo(VI) framework structures. In the bioctahedral unit, the two $Mo^{VI}O_6$ octahedra exhibit a staggered configuration and the Mo(1)−O(10)−Mo(2) bond angle is 137.0(3)°. On the other hand, the diarsenate groups linked to the Mo_2O_{11} units are strictly eclipsed as compared with the staggered configurations often encountered in the other transition metal diarsenate structures.[13] In the IR spectrum, two bands centered at 569 and 769 cm^{-1} are attributed to the symmetric and asymmetric As−O−As vibration modes of As_2O_7. In addition, the As−O stretching frequencies associated with the [AsO_4] can be observed at 828, 851, 893, and 905 cm^{-1}. These values are consistent with the characteristic bands for $Na_4As_2O_7$.[14]

The structure of **2** contains the known $[Mo_4O_{10}(HAsO_4)_4]^{4-}$ anion,[15] which is formed of two edge-sharing bioctahedral Mo_2O_{10} units[16] and four tetrahedra of the $HAsO_4$ groups. Each of the $[Mo_4O_{10}(HAsO_4)_4]^{4-}$ anions is connected to four others via strong hydrogen bonds to form anion layers running parallel to the (101) planes (Figure 4). Connections between adjacent layers are solely provided by O−Cs−O bonds. In comparison with the isostructural compound $[C_5H_5NH]_2Mo_2O_5(HAsO_4)_2$·

(11) Meier, W. M.; Olson, D. H. *Atlas of Zeolite Structure Types*; Butterworth-Heinemann: Stoneham, MA, 1992.
(12) (a) Canadell, E.; Provost, J.; Guesdon, A.; Borel, M. M.; Leclaire, A. *Chem. Mater*. **1997**, *9*, 68. (b) Lii, K. H.; Wang, C. C. *J. Solid State Chem*. **1988**, *77*, 117. (c) Costentin, G.; Leclaire, A.; Borel, M. M.; Grandin, A.; Raveau, B. *Rev. Inorg. Chem*. **1993**, *13*, 77.
(13) Chen, T. C.; Wang, S. L. *J. Solid State Chem*. **1996**, *121*, 350. (b) Wang, S. L.; Wu, C. H.; Liu, S. N. *J. Solid State Chem*. **1994**, *113*, 37.
(14) Nakamoto, K. In *Infrared and Raman Spectra of Inorganic and Coordination Compounds*, 4th ed.; Wiley: New York, 1986.
(15) Takeuchi, Y.; Kobayashi, A.; Sasaki, Y. *Acta Crystallogr., Sect. B* **1982**, *38*, 242.
(16) Several reduced Mo_2O_{10} bioctahedral units can be found in the following references: (a) Guesdon, A.; Leclaire, A.; Borel, M. M.; Raveau, B. *J. Solid State Chem*. **1996**, *122*, 343. (b) Guesdon, A.; Leclaire, A.; Borel, M. M.; Grandin, A.; Raveau, B. *J. Solid State Chem*. **1995**, *114*, 481. (c) Minoli, L. A.; Haushalter, R. *Inorg. Chem*. **1990**, *29*, 2879.

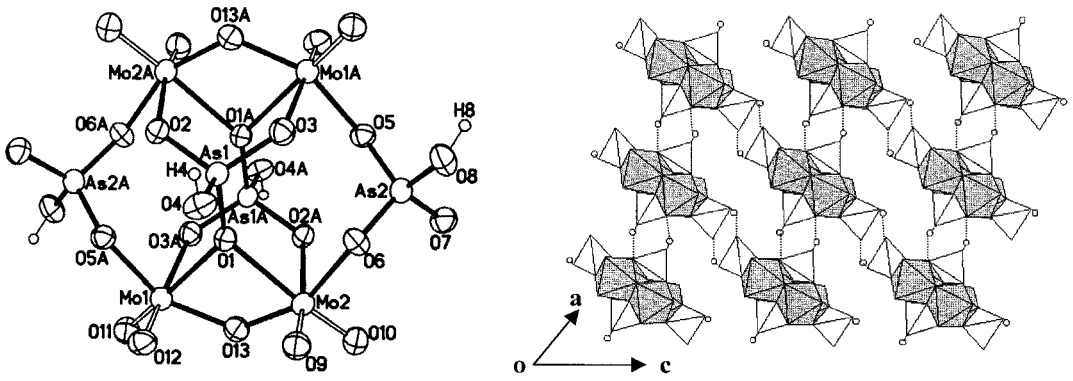

Mo1-O11	1.683(8)	Mo1-O5A	1.989(5)	Mo2-O10	1.705(6)	Mo2-O6	2.012(7)
Mo1-O12	1.708(5)	Mo1-O3A	2.226(5)	Mo2-O9	1.715(5)	Mo2-O2A	2.230(4)
Mo1-O13	1.921(5)	Mo1-O1	2.320(7)	Mo2-O13	1.891(7)	Mo2-O1	2.344(5)
As1-O1	1.695(7)	As1-O3	1.663(6)	As2-O5	1.685(4)	As2-O7	1.662(6)
As1-O2	1.682(4)	As1-O4	1.729(5)	As2-O6	1.683(5)	As2-O8	1.709(8)

Figure 4. Structure plots of **2**. (Left) ORTEP drawing (50% ellipsoids) of the $[Mo_4O_{10}(HAsO_4)_4]^{4-}$ anion with atomic labeling and selected bond lengths. (Right) polyhedron representation displaying the packing of the anions along [010]. H bonds are presented in dotted lines.

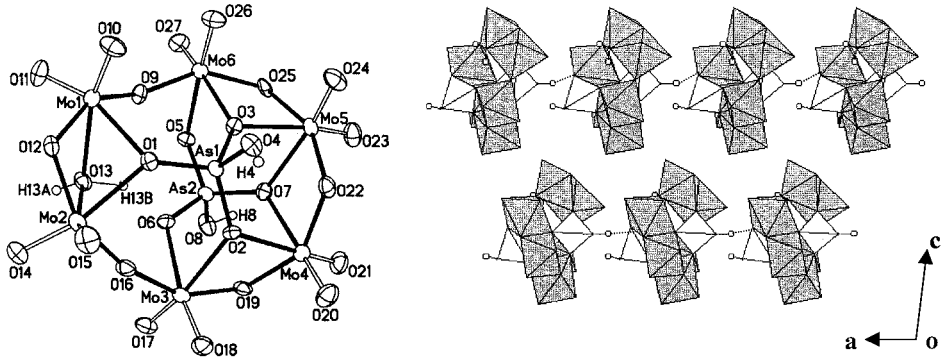

Mo1-O11	1.700(8)	Mo1-O12	1.946(7)	Mo2-O14	1.692(8)	Mo2-O12	1.941(7)
Mo1-O10	1.703(8)	Mo1-O1	2.287(7)	Mo2-O15	1.723(8)	Mo2-O1	2.307(7)
Mo1-O9	1.878(7)	Mo1-O13	2.400(7)	Mo2-O16	1.865(8)	Mo2-O13	2.433(7)
Mo3-O18	1.703(8)	Mo3-O19	1.929(7)	Mo4-O20	1.705(8)	Mo4-O22	1.924(8)
Mo3-O17	1.708(8)	Mo3-O6	2.278(7)	Mo4-O21	1.710(8)	Mo4-O7	2.284(7)
Mo3-O16	1.927(8)	Mo3-O2	2.318(7)	Mo4-O19	1.917(7)	Mo4-O2	2.371(7)
Mo5-O24	1.704(8)	Mo5-O22	1.939(8)	Mo6-O26	1.699(8)	Mo6-O25	1.925(8)
Mo5-O23	1.709(9)	Mo5-O7	2.275(7)	Mo6-O27	1.706(7)	Mo6-O5	2.292(7)
Mo5-O25	1.938(7)	Mo5-O3	2.283(7)	Mo6-O9	1.922(7)	Mo6-O3	2.355(7)
As1-O1	1.683(7)	As1-O3	1.679(7)	As2-O5	1.673(7)	As2-O7	1.693(7)
As1-O2	1.683(7)	As1-O4	1.723(7)	As2-O6	1.676(7)	As2-O8	1.709(8)

Figure 5. Structure plots of **3**. (Left) ORTEP drawing (50% ellipsoids) of the $[Mo_6O_{18}(H_2O)(HAsO_4)_2]^{4-}$ anion with atomic labeling and selected bond lengths. (Right) polyhedron representation displaying the packing of the anions along [010]. H bonds are presented in dotted lines.

H_2O,[17] **2** shows no H bond interactions between lattice water and anions. In addition, the TG curve of **2** does not reveal the weight loss corresponding to O_2 and As_2O_3 as observed in the pyridinium salt. The thermal behavior of the $[Mo_4O_{10}(HAsO_4)_4]^{4-}$ anion is strongly cation-dependent as shown by the two isostructures.

The structure of **3** contains the larger molecular cluster anion, $[Mo_6O_{18}(H_2O)(HAsO_4)_2]^{4-}$, which is composed of six MoO_6 octahedra to form a ring by sharing one face, two corners, and three edges and of two tetrahedral $HAsO_4$ groups capped on opposite sides of the ring, one from above and the other from below. It is topologically identical to $[(RAs)_2Mo_6O_{25}H_2]^{4-}$ (R = Me, Ph, *p*-$C_6H_4NH_2$),[18] from which various heteropolyanions with different molybdenum to hetero parts could be generated by varying pH in solution. When the R groups are replaced by hydroxyl groups, it becomes the $[Mo_6O_{18}(H_2O)(HAsO_4)_2]^{4-}$ anion in **3**. Materials which contain such an anion have not been isolated before. Another topologically similar cluster anion, $[HMo_6As_2O_{26}]^{5-}$, was also reported.[19] It carries one more negative charge and the six MoO_6 octahedra are joined to each other by common edges only. It was noted that dehydration of **3** was completed at ~240 °C, which is rather low as compared with **2** or other $HAsO_4$-containing materials. A number of

(17) Wang, S. L.; Hsu, K. F.; Nieh, Y. P. *J. Chem. Soc., Dalton Trans* **1994**, 1681.

(18) (a) Pope, M. T.; Mueller, A. *Angew. Chem., Int. Ed. Engl.* **1991**, *30*, 34. (b) Takahama, H. Yagasaki, A. Sasaki, Y. *Chem. Lett. Chem. Soc. Jpn.* **1982**, 1953. (c) Matsumoto, K. *Bull. Chem. Soc. Jpn.* **1978**, *51*, 492. (d) Kwak, W.; Rajkovic, L. M.; Pope, M. T.; Quicksall, C. O. *J. Am. Chem. Soc.* **1977**, *99*, 6463. (e) Kwak, W.; Rajkovic, L. M.; Stalick, J. K.; Pope, M. T.; Quicksall, C. O. *Inorg. Chem.* **1976**, *15*, 2778.

(19) Hedman, B. *Acta Crystallogr., Sect. B* **1982**, *36*, 2241.

strong hydrogen bonds between adjacent $[Mo_6O_{18}(H_2O)(HAsO_4)_2]^{4-}$ cluster anions, especially along the ⟨100⟩ directions (Figure 5), may account for the lower dehydration temperature.

Conversion of the cluster anions $[Mo_4O_{10}(HAsO_4)_4]^{4-}$ and $[Mo_6O_{18}(H_2O)(HAsO_4)_2]^{4-}$ into the framework of **1** should involve two major steps: (1) formation of the As_2O_7 units by condensation of the $HAsO_4$ groups, and (2) cleavage of edge- or face-shared Mo−O bonds in **2** and **3**. As revealed in Figures 4 and 5, strong H bonds between the cluster anions facilitate the completion of the first step. The smaller endothermic peaks marked with arrows in the DT curves of **2** and **3** (Figure 1) correspond to this condensation process. The second step occurs primarily within the individual cluster anion. In $[Mo_4O_{10}(HAsO_4)_4]^{4-}$, breaking of the longest Mo−O(1) bonds will result in the corner-shared bioctahedral Mo_2O_{11} units as characterized in **1**. This bond-breaking process accounts for the broad endothermic peak at ca. 465 °C in the DT curve of **2**. In $[[Mo_6O_{18}(H_2O)(HAsO_4)_2]^{4-}$, many more Mo−O bonds are to be cleaved in order to form the discrete Mo_2O_{11} units. The detailed bond-breaking and rearrangement processes are not completely understood so far. Nontheless, the sharp endothermic peak occurred at ca. 525 °C in the DT curve of **3** illustrates the occurrence of such processes.

The lattice water in **1** is originated from humidity. As indicated by TG analysis, the water was evolved completely below 50 °C. As compared with the less open framework phosphate $Cs_6Mo_7O_9(PO_4)_7 \cdot H_2O$ (FD = 14.9 M),[2b] in which water molecules also came from atmosphere and were released at 500 K, the reversible hydration−dehydration process takes place more readily in **1**. Furthermore, a polymorph might have emerged as the dehydration of **1** showed a sharp endothermic peak at ∼650 °C in the DT curve without a counterpart in the TG curve. It should be very interesting to obtain the crystal structure of any polymorph of **1**.

This work has important implications for the conversion of discrete cluster anions into three-dimensional network.[20] The synthetic approaches adopted here may provide a convenient, perhaps a better route for the preparation of a specific heteropolyanion than solution chemistry. By varying the compositon of the flux, different sizes of cluster anions may be generated. The combined studies of thermal analysis and X-ray structures confirm the first experimental observation of a metal diarsenate framework being thermally converted from hydrogen arsenate-containing materials. Further invetigations employing both hydrothermal and flux-growth methods for the preparation of open-framework solids will be undertaken.

Acknowledgment. We thank the National Science Council of the Republic of China for support of this work (NSC87-2113-M-007-015).

Supporting Information Available: X-ray crystallography data including tables of complete crystal data, atomic coordinates, bond distances and angles, anisotropic thermal parameters, X-ray powder patterns, and TGA/DTA diagrams for $Cs_2Mo_2O_5As_2O_7 \cdot H_2O$, $Cs_2Mo_2O_5(HAsO_4)_2 \cdot H_2O$, and $Cs_4Mo_6O_{18}(H_2O)(HAsO_4)_2 \cdot 2.5H_2O$ (13 pages). Ordering information is given on any current masthead page.

IC971562V

(20) (a) Stein, A.; Keller, S. W.; Mallouk, T. E. *Science* **1993**, *259*, 1558. (b) Whitesides, G. M.; Mathias, J. P.; Seto, C. T. *Scienc*e **1991**, *254*, 1312. (c) Lehn, J. M. *Angew Chem., Int. Ed. Engl.* **1988**, *27*, 89.